RP Current Trends In Applied Sciences (e-ISSN: 2583-7486)
Vol. 5, No. 2 (April – June 2026) pp. 71–78

RESEARCH PLATEAU PUBLISHERS

Cite this article: R. Dhayalan, Generation and detection of ultrasonic shear horizontal plate waves in thick low carbon steel plates using magnetostrictive EMAT, *RP Cur. Tr. Appl. Sci*. **5** (2026) 71–78.

Original Research Article

Generation and detection of ultrasonic shear horizontal plate waves in thick low carbon steel plates using magnetostrictive EMAT

R. Dhayalan*

Non-Destructive Evaluation Division, Indira Gandhi Centre for Atomic Research, Kalpakkam-603 102, Tamil Nadu, India
*Corresponding author, E-mail: dhayalanr@gmail.com

ARTICLE HISTORY
Received: 16 April 2026
Revised: 27 May 2026
Accepted: 27 May 2026
Published: 13 June 2026

KEYWORDS
Shear horizontal plate waves; Magnetostrictive EMAT; Low carbon steel plate; Finite element simulation; Dispersion curves; Time-Frequency analysis.

ABSTRACT
Ultrasonic shear horizontal (SH) plate waves are useful in nondestructive testing (NDT) applications because of their simple dispersion characteristics. Electromagnetic acoustic transducers (EMAT) are ideal for generating these waves and particularly attractive for probing steels and its alloys because their transduction efficiency is larger than in non-ferromagnetic materials. The objective of this work is to investigate low frequency SH plate wave transduction in thick low carbon steel plates by using magnetostrictive EMATs. In this study, magnetostrictive EMATs were designed using elongated spiral racetrack coils in conjunction with periodic permanent magnets (PPM), featuring a magnet periodicity (wavelength) of 6 mm. The excitation frequency of this EMAT was optimized and tuned at 600 kHz to generate these waves on 5 mm and 10 mm thick carbon steel plates. The generated SH plate wave modes were analyzed with the help of time-frequency analysis and dispersion curves. The potential of these wave modes was also examined to detect artificial defects made on both carbon steel plates. From the characteristics of transmission and reflection of these waves in thick carbon steel plates with artificial defects, it was observed that the low frequency SH guided waves can effectively detect defects of 10% wall thickness in thick carbon steel plates. It was noted that the excitation frequency of this EMAT was low, however it could effectively detect defects in thick carbon steel plates with high sensitivity.

1. Introduction

Electromagnetic acoustic transducers (EMATs) offer several significant advantages over conventional piezoelectric based transducers for ultrasonic non-destructive testing (NDT) [1-3]. These advantages include: (i) non-contact (no need of liquid couplant) wave generation (ii) the ability to generate waves in any desired direction within the test specimen through the strategic selection of EMAT design configuration, (iii) ease of fabrication and greater compatibility compared to other ultrasonic transducers, and (iv) the capability to generate all types of sound waves including shear horizontal (SH) waves, which are challenging to excite using conventional piezoelectric based transducers [4-6]. The capability of EMATs to excite SH waves enables the exploitation of their unique characteristics in ultrasonic testing. As these waves are polarized parallel to the exciting surface of the test specimen, they are excited by the transverse stress produced by the transducer without any side lobes as head, compressional, and Rayleigh or surface waves. At normal incidence, SH waves are completely reflected without mode conversion from an edge or defect [6, 7].

SH-plate waves are a type of ultrasonic guided or plate wave. These waves can travel through plate-like structures that are thinner than a few wavelengths [8]. In an infinite plate structure free from stress, these waves manifest as 2-D stress waves [9]. Their propagation characteristics are specifically influenced by the geometry of the structure being inspected. The elastic motion of these waves covers the entire thickness of the structure, guided by the top and bottom surfaces of the plate. SH-plate waves experience minimal divergence losses and are less attenuated than ultrasonic bulk waves, allowing them to propagate over longer distances at the same frequency, which enhances their sensitivity for detecting defects [10]. Additionally, these waves are particularly sensitive to adhesion defects, such as disbonds between the coating and the plate surface, areas where corrosion is frequently a problem [11]. The basic oscillation pattern of the fundamental SH wave (SH0) is shown in Figure 1. For the SH0-mode, lattice motion is perpendicular propagation direction and parallel to the material surface.

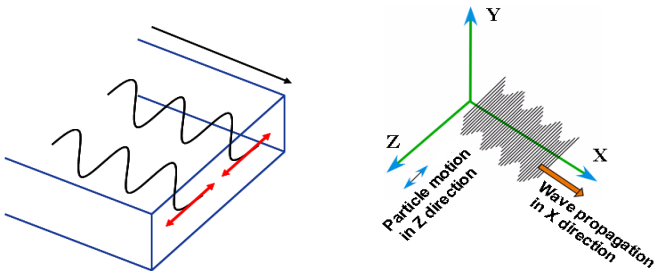

Figure 1: Displacement pattern of SH waves.

EMATs are capable of exciting and/or receiving ultrasonic waves in magnetic materials via the magneto-elastic effect or magnetostriction, and in non-magnetic materials via the Lorentz force principle [12-14]. In this study, the material

under examination is magnetic, specifically a low carbon steel plate, where the EMAT operates through a combination of magnetostriction, Lorentz force, and magnetization effects. The magnetostrictive effect is significantly high in low-carbon steel, where magnetic domains align and cause the material to strain under a magnetic field [15]. Low carbon steel plates are commonly used in nuclear and conventional industries because they are easy to weld, flexible, and affordable. In nuclear industries, they are often used for containment vessels, structural components storage tanks, and auxillary piping [16]. Beyond nuclear applications, these plates are widely employed in constructions, shipbuilding, automotive, and fabrication of pressure vessels [17].

An EMAT typically comprises of a high-frequency coil and a permanent magnet, which can function as either a detector or a generator of ultrasonic waves. In the generation mode, an alternating current (AC) passing through the coil creates a dynamic magnetic field that interacts with the bias field, leading to the periodic rotation of magnetic domains [18]. This interaction induces cyclic strain in the material due to magnetostriction, thereby generating ultrasonic waves within the plate. The bias field provided by the permanent magnet enhances the efficiency of wave generation [19]. A significant advantage of the magnetostrictive principle in low carbon steel plate is the ease of generating low-frequency SH plate waves. By selecting a racetrack or elongated spiral coil with an array of periodic permanent magnets (PPM), EMATs can produce magnetostrictive strains that facilitate the generation and detection of SH plate waves [20].

The prime objective of this paper is to develop magnetostrictive EMATs using elongated spiral coils and PPM for generating SH plate waves in low carbon steel plates. To optimize the EMAT design configurations, a series of 3-D finite element (FE) models were created to demonstrate the generation of SH plate waves in low carbon steel plates. Using these EMAT, low frequency SH plate waves were generated in low carbon steel plates of two different thicknesses and analyzed by using the dispersion curves and time-frequency analysi. Finally, the experimental measurements were compared with FE simulation results and the magnetostrictive EMATs were also used to demonstrate defect detection in low carbon steel plates.

2. Finite element (FE) simulation of magnetostrictive EMAT

Considerable research works have been reported earlier on development of different types of EMAT configurations to generate SH waves for various NDT applications [2-4]. Most of the EMATs were utilized to generate angle beam SH bulk waves and plate waves for defect detection and weld inspection in austenitic stainless-steel plates and pipes [5, 6]. Most of the analytical and simulation studies on the SH wave EMATs were carried out in two dimensions, by considering the plane in which the SH wave oscillates [18-20]. In this paper, three-dimensional (3D) FE modelling of a magnetrostrictive EMAT was performed in two phases. Initially, an electromagnetic model was designed to calculate for the body forces inside the magnetic material. The commercial FE package COMSOL® was utilized for the electromagnetic modelling of magnetrostrictive EMAT. Subsequently, ultrasonic wave propagation simulation was carried out by using another explicit FE tool ABAQUS. The values of body forces obtained from the electromagnetic model were used as the inputs for the ultrasonic wave propagation model. The top and cross-sectional views of the 3-D magnetostrictive EMAT transmitter are shown in Figure 2(a) and 2(b).

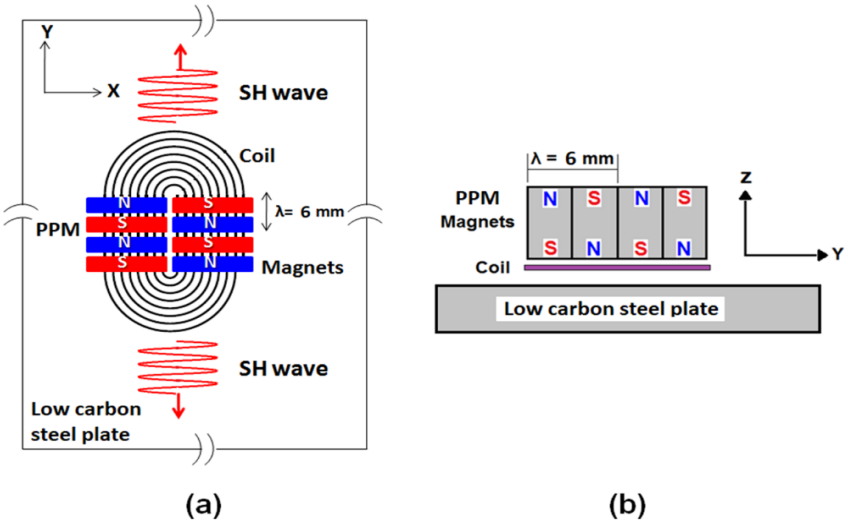

Figure 2: Arrangement of race-track coil, magnetic array and the test specimen (a) top view and (b) cross-sectional view.

The arrangement of the elongated spiral coil, array of PPM, and low carbon steel plate are shown in both figures. In Figure 2(b), the alternate magnet spacing or periodicity in PPM is equivalent to one wavelength (λ). Neodymium-Iron-Boron (Nd-Fe-B) magnets were chosen with flux density of 0.4 T. Copper was chosen for the excitation coil which was designed as an elongated spiral with 8 number of turns and 2.0 mm line spacing. When the coil was excited with a high alternating current pulse in transmission mode, PPM induced alternating static magnetic fields within the skin depth (one wavelength) of the low-carbon steel plate below the coil and PPM. The alternating current induced eddy currents and dynamic magnetic fields within the plate's skin depth. In alternating bias fields, these induced currents and dynamic fields produced body forces (Lorentz force, magnetization, and magnetostrictive forces) within the skin depth. The transient body forces inside the plate below each magnet in PPM alternates at the driving current's frequency, acting as the

ultrasonic waves' source. By applying these forces in ultrasonic wave propagation model, time dependent elastic stress waves were generated inside the plate. Figure 3(a) and 3 (b) show the screenshots of 3D electromagnetic COSMSOL model and wave propagation ABAQUS model respectively. The derivation of electromagnetic and acoustic equations for modeling the meander coil EMAT to generate bulk waves, Rayleigh waves and Lamb wave generation have already been discussed in more detail elsewhere [21].

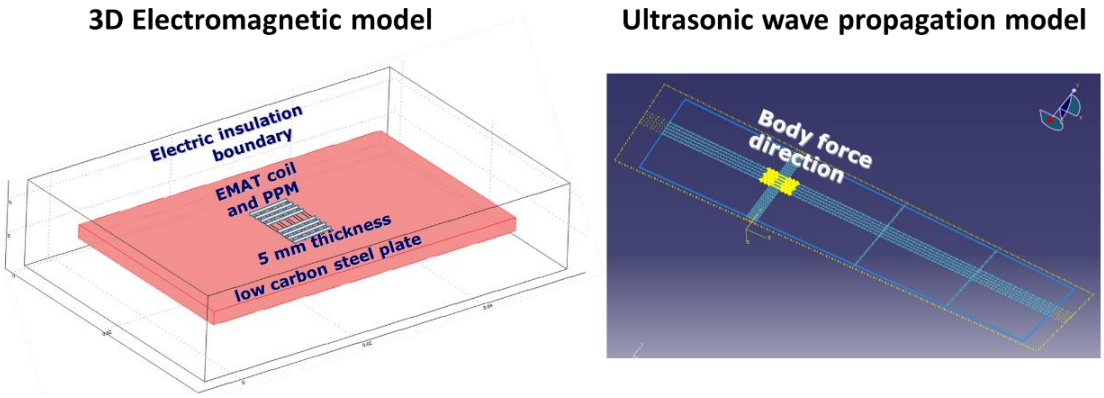

(a) (b)

Figure 3: Snapshots obtained from (a) the electromagnetic (COMSOL) model and (b) wave propagation (ABAQUS) model.

3. Design consideration and experimental details

The magnetostrictive EMATs were developed with elongated spiral coils and array of PPM for the experimental measurements. Figure 4 shows the photograph of the developed SH wave EMAT with a PPM array to generate the SH plate waves in low carbon steel plates. For optimum design consideration, the excitation coil and the magnets are the required components and its geometrical features determines the generation of wave modes. These coils were made using a flexible PCB technique which provided to design any arbitrary design with high accuracy. The printed circuits boards were made from 200-µm flexible polyester laminate with 100 µm thick copper clad. The total thickness of the sheet was 300 µm. The permanent magnets in PPM array were Nd-Fe-B sintered magnets that exhibited flux density, B, at the metal surface of nearly 0.4 T. The magnet array consisted of eight magnets and the dimension of each magnet was 15×10×6 mm. The EMAT were developed with the same design parameters as used as in simulation studies.

Figure 4: Photograph of the SH wave EMATs with elongated spiral coils and array of periodic permanent magnets (PPM).

The alternate polarity of the permanent magnets causes the tangential body force distribution whose directions alternately change with the same period of the magnet array. Depending upon the frequency of excitation, such a body force distribution generates the shear waves polarized parallel to the specimen surface in both sides. The generation of SH plate wave mode depends upon the size of the magnet and the material thickness. The maximum transfer efficiency occurs when the wavelength is tuned to the spacing or size of the magnets. Hence, the size of the magnet or period of the magnet array (λ) was 6 mm which was equalant to the wavelength of the excited SH plate wave modes. Figure 5 shows the schematic and photograph of the instrumentation set up used for the experimental studies.

To achieve a high-power RF tone burst, a RITEC RPR4000 gated amplifier was employed. A power matching network was utilized to enhance the EMAT coil current by aligning the relatively high output impedance of the RITEC amplifier with the typically lower coil impedance. The system's signal-to-noise ratio (SNR) was enhanced by aligning the usually low impedance of the receiver coil with the higher impedance of the receiver amplifier. Signals were captured using the Yokogawa, DL9140 digital storage oscilloscope for data archiving and subsequent analysis. Prior to commencing the actual experiment, all instruments and the power level of the RITEC amplifier, along with the control settings, were verified and calibrated.

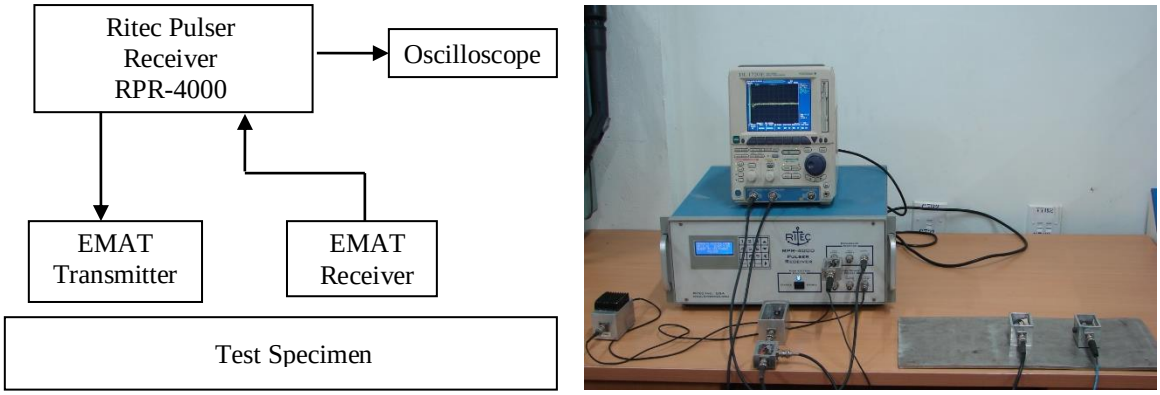

Figure 5: Schematic diagram and photograph of the experimental set-up.

4. Generation and detection of SH plate waves in low carbon steel plate

The low frequency SH plate waves were generated and detected in two low carbon steel plates of same size i.e., 700 mm in length, 500 mm wide with thicknesses of 5 mm and 10 mm. The measurements were carried out using separate transmitter and receiver (through transmission method). A peak current of about 40 ampere was fed to the transmitter EMAT to excite the plate waves. The signals were received by another identical EMAT. It is well established that to identify the SH plate wave modes that can be generated using an EMAT, it is necessary to examine the dispersion characteristics, velocity of individual wave modes and excitation frequency [22]. A commercial software tool, DISPERSE®, was employed to plot dispersion curves for these plates. Figure 6 presents the group and phase velocity dispersion curves of low carbon steel plate for various modes as a function frequency versus velocity. The relatively non-dispersive, low frequency region (up to 1 MHz) is indicated as blue dotted rectangular box on the left side of the dispersion curves. The highly dispersive region (above 1 MHz) is highlighted on the right side of the dispersion curves.

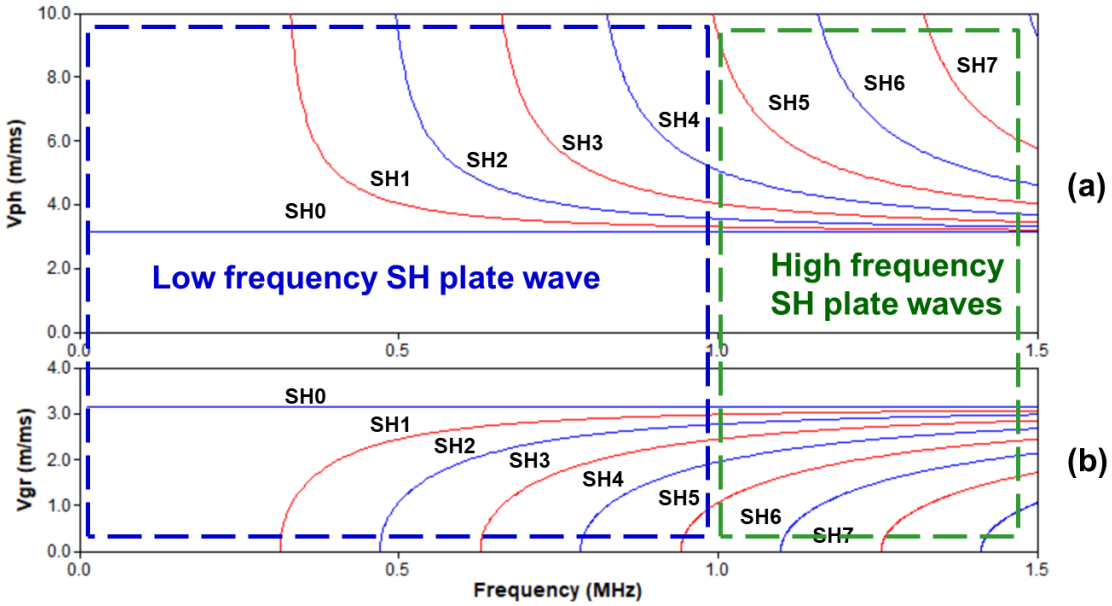

Figure 6: SH wave dispersion curves for low carbon steel plate: (a) phase velocity and (b) group velocity curves.

In order to optimize the frequency for generating the low frequency SH plate waves on both low carbon steel plates, the excitation frequency was swept for a wide frequency range from 100 kHz to 1 MHz. Figure 7(a) shows the measurement setup employed for the generation of SH plat waves using EMAT; this configuration was same for both experimental measurements and simulations. The transmitter EMAT was located on the flat surface of the plate and the receiver center was positioned 125 mm away from the transmitter center. The receiver EMAT was oriented along the axis of the wave front generated by the transmitter EMAT. For FE simulations, a series of 3D models were developed for a frequency from 100 kHz to 1 MHz to generate SH plate waves on both the plates. The optimum frequency of generating the SH plate waves for each plate was obtained by frequency sweep method. The amplitude response of the SH plate waves was monitored when the excitation frequency swept from low to high. For each plate, initially the amplitude of SH plate wave was increased with increase in frequency and attained a maximum called peak or optimum frequency. It was observed that the maximum amplitude response of the low frequency SH plate wave modes on both plates was 600 kHz. The amplitude response of the SH waves in simulation output exactly follows the same trend line of the experimental outputs for both the plates. Figures 7(b) and 7(c) show the SH plate wave amplitude response of both experimental and simulation outputs on both 5- and 10-mm thickness low carbon steel plates.

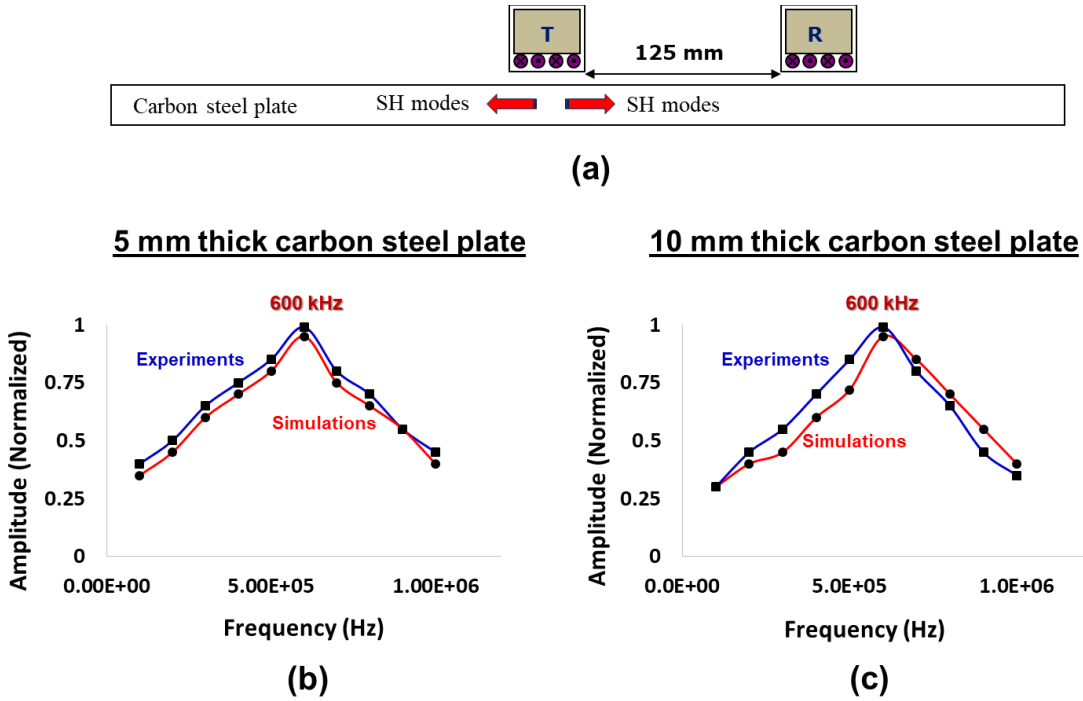

Figure 7: (a) Measurement set-up used for the generation of SH plate waves and the amplitude responses of SH plate waves on low carbon steel plates of (b) 5 mm thickness and (c) 10 mm thickness.

The time-amplitude A-scan signals of SH plates obtained at the optimum frequency of 600 kHz from the experimental measurements and FE simulations on both low carbon steel plates are shown in Figure 8(a) and 8(b). It was noted that the amplitude response of SH plate was more for thinner plate. The number of SH plate wave modes are more in thicker plate than the thinner plate. From Figure 8, it was observed that the experimental results are in line with the FE simulation results in terms of mode shapes, number of SH wave modes present in the A-scan signals.

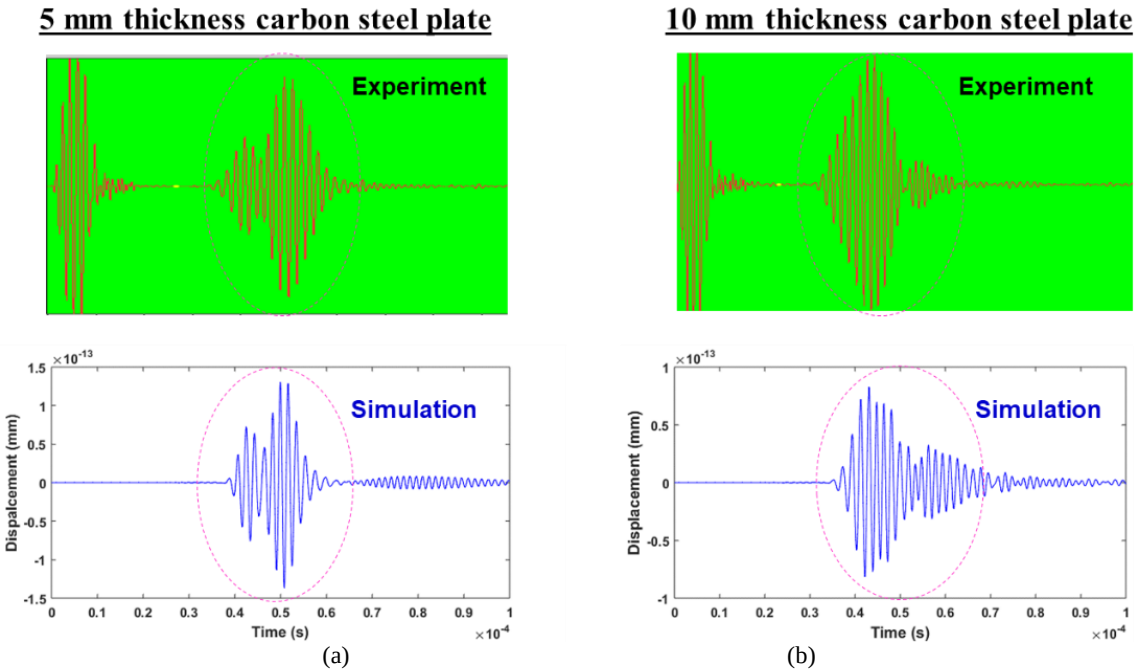

Figure 8: Comparison of time-amplitude SH plate waves obtained from the experiments and FE simulations on low carbon plate of (a) 5 mm thickness and (b) 10 mm thickness.

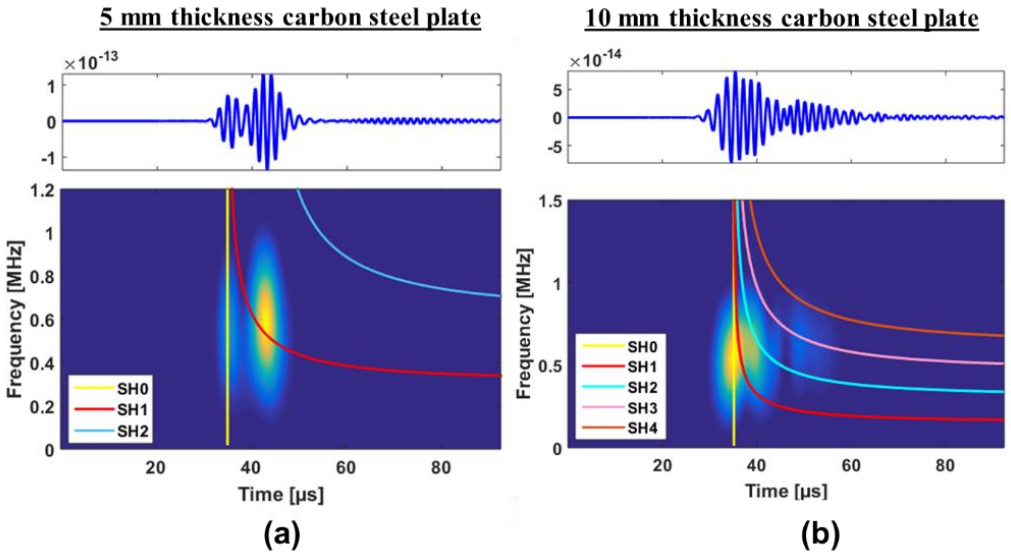

Figure 9: Time-frequency (STFT) representation SH plate waves in low carbon steel plate of (a) 5 mm thickness and (b) 10 mm thickness.

The SH modes associated with low-frequency plate waves were analyzed using the time-frequency or short-time Fourier transform (STFT), aided by group velocity dispersion curves plotted for both plates. A comprehensive explanation of the STFT can be found in [23]. Figures 9(a) and 9(b) depict the superposition of STFT with SH wave dispersion curves for both plates. The SH plate wave modes identified in the A-scan signal obtained from the 5 mm thickness plate are SH0 and SH1. Similarly, the SH plate wave modes present in the 10 mm thickness plate are SH0, SH1, SH2, SH3 and SH4.

5. Testing of defect using SH plate waves

The SH plate waves, generated by the magnetostrictive EMAT, were also utilized to detect artificial defects in both carbon steel plates. To demonstrate the capabilities of the low-frequency SH plate waves, three electric discharge machined (EDM) notches, each 10 mm long and 1 mm wide, with varying depths (10%, 20%, and 30% of wall thickness), were created on both plates at a distance of 100 mm from one edge. Each notch was laterally separated by 100 mm. Figure 10 illustrates the schematic of the measurement setup used for defect detection with SH plate waves in carbon steel plates of 5 mm and 10 mm thickness.

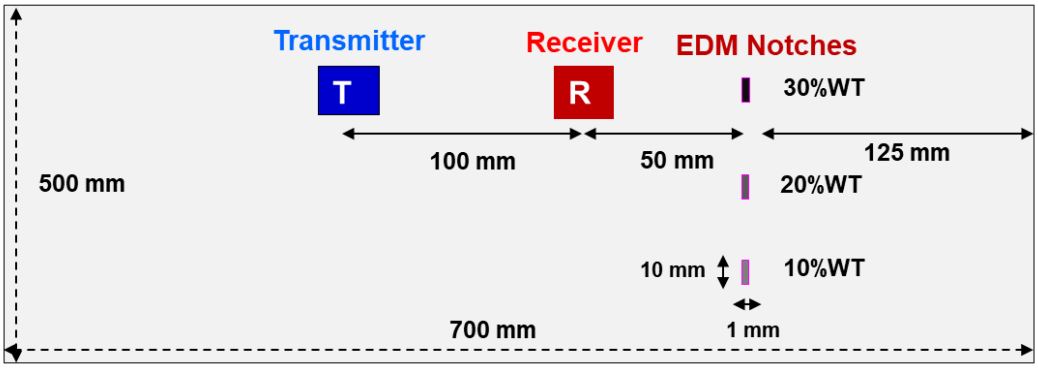

Figure 10: Schematic diagram test set up for defect detection in 5 mm and 10mm thickness plates using SH plate waves.

In order to detect the defects in both low carbon steel plates, the magnetostrictive EMAT was excited at the optimal frequency of 600 kHz. Utilizing the setup depicted in Figure 10, SH plate waves were generated and directed to interact with all the EDM notches present in both steel plates. The reflected waves were then captured, with the results illustrated in Figures 11 and 12. In these results, the initial signals detected are the direct transmissions from the transmitter, followed by signals are reflected from the defects. Due to the finite dimensions of the transmitter and receiver, reflections from the plate's edges were also captured. It was noted that the amplitude of the defect signal increases with the defect's depth, while the amplitude of the edge reflection diminishes as the defect size increases.

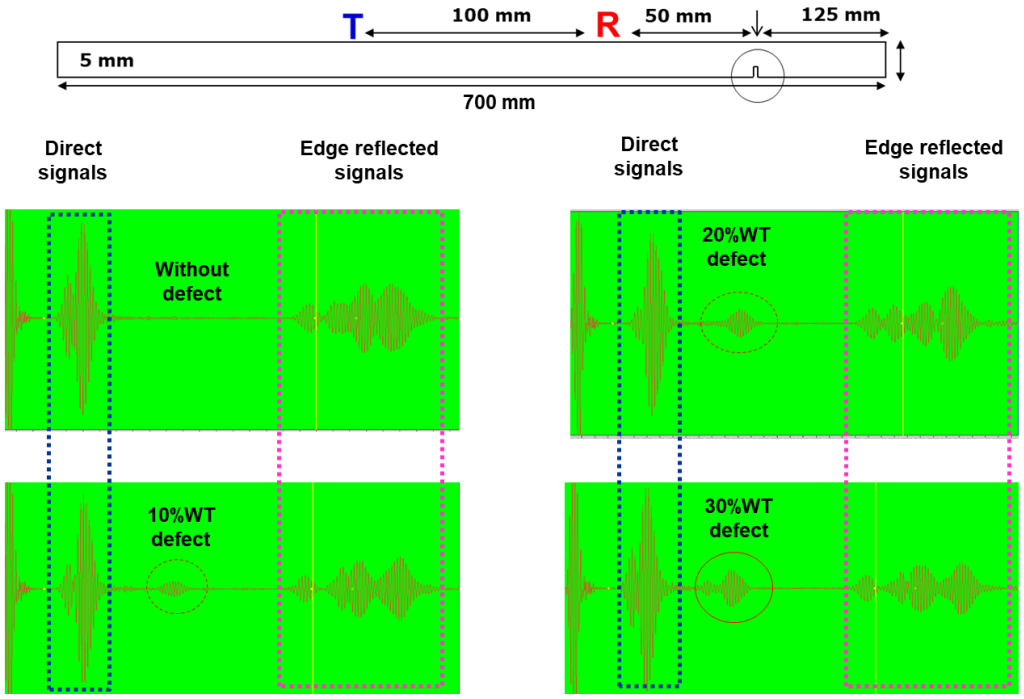

Figure 11: Detection of defects (EDM notches) using SH plate waves in 5 mm thickness carbon steel plate.

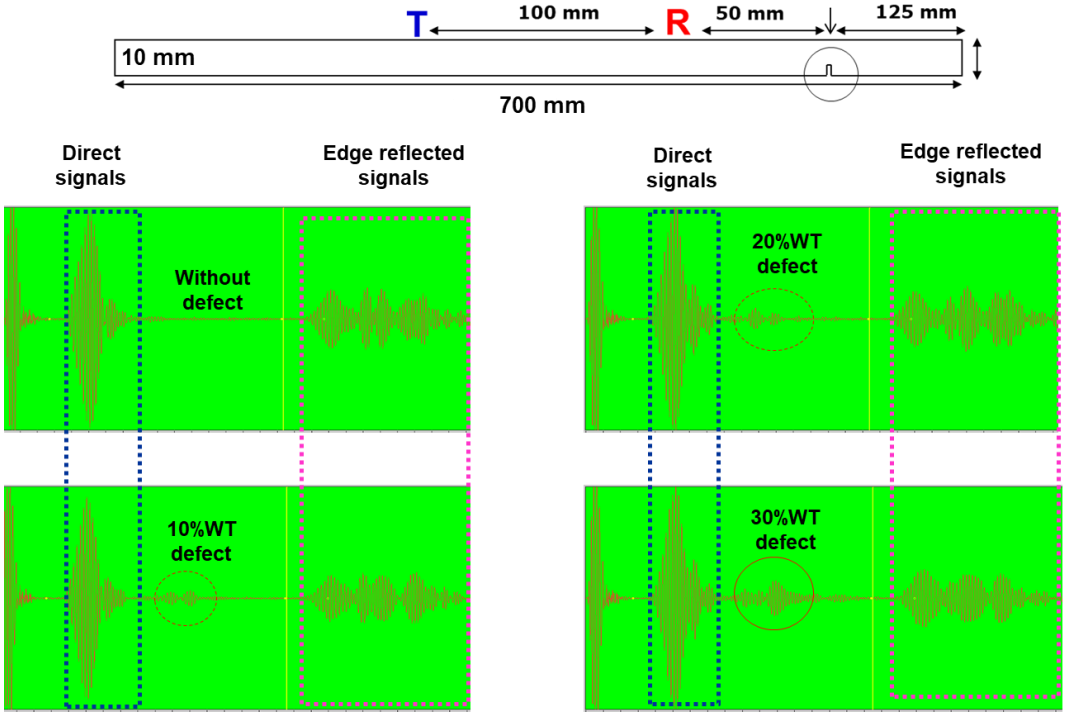

Figure 11: Detection of defects (EDM notches) using SH plate waves in 10 mm thickness carbon steel plate.

6. Summary and conclusions

Magnetostrictive EMATs were developed to generate and detect SH plate wave modes in low carbon steel plates. These EMATs were designed by using elongated spiral coil and an array of PPM and those performance were assessed through both FE simulations and experimental tests. In the FE simulation, 3-D electromagnetic models were designed for the body force calculations inside the steel plate. Further, these body forces were utilized in an acoustic model as the excitation forces to generate the SH plate waves in carbon steel plate. For experimental measurements, the elongated spiral coils were made using flexible PCB copper coils and 3 mm thick Nd-Fe-B permanent magnets. All of the measurements were carried out with magnetostrictive EMAT on low carbon steel plates of 5 mm and 10 mm thickness. The optimal frequency for this EMAT was measured by frequency sweep method. The amplitude of SH plate wave modes increased with frequency, reaching a maximum before decreasing with further frequency increases. The optimum frequency of SH plate waves was found to be 600 kHz for both steel plates. The generated SH plate wave modes were analyzed and identified using time-frequency analysis (STFT) and dispersion curves. It was found that the amplitude of SH plate wave modes generated in the thin plate was higher than in the thicker plate. However, the

number of wave modes involved in the SH plate waves was greater in the thicker plate than in the thinner one. The SH plate waves were also used to detect artificial defects in both carbon steel plates, with the amplitude of the defect signals increasing with the size of the defect.

Authors' contributions

The author read and approved the final manuscript.

Conflicts of interest

The author declares no conflict of interest.

Funding

This research received no external funding.

Data availability

No new data were created.

References

[1] R.B. Thompson, Physical principles of measurements with EMAT transducers, in: R.N. Thurston, A.D. Pierce (Eds.), Physical Acoustics, Vol. 19, Academic Press, San Diego (1990).
[2] M. Hirao, H. Ogi, EMATs for Science and Industry: Noncontacting Ultrasonic Measurements, Kluwer Academic Publishers (2003).
[3] G.A. Alers, L.R. Burns, EMAT designs for special applications, *Mater. Eval*. **45** (1987) 1184–1189.
[4] M. Hirao, H. Ogi, An SH-wave EMAT technique for gas pipeline inspection, *NDT&E Int.* **32** (1999) 127–132.
[5] K. Sawaragi, H.J. Salzburger, G. Hübschen, K. Enami, A. Kirihigashi, N. Tachibana, Improvement of SH-wave EMAT phased array inspection by new eight segment probes, *Nucl. Eng. Des*. **198** (2000) 153–163.
[6] R. Dhayalan, A. Kumar, C.K. Mukhopadhyay, EMAT-phased array inspection of thick austenitic stainless steel and dissimilar metal welds, in: C.K. Mukhopadhyay, R. Mulaveesala (Eds.), Advances in Non-destructive Evaluation, Lecture Notes in Mechanical Engineering, Springer, Singapore (2021).
[7] M. Spies, Computationally efficient SH-wave modeling in transversely isotropic media, *J. Nondestruct. Eval*. **19** (2000) 2–12.
[8] J.L. Rose, Guided wave nuances for ultrasonic nondestructive evaluation, *IEEE Trans. Ultrason. Ferroelectr. Freq. Control* **47** (2000) 575–583.
[9] W. Luo, J.L. Rose, Guided wave thickness measurement with EMATs, *Insight* **45** (2003) 11–16.
[10] Q. Li, et al., A method of shear-horizontal EMAT based on dual-reception magnetic encoded spatial pulse compression for multiple cracks identification and location, *IEEE Magn. Lett*. **14** (2023) 1–5.
[11] K. Arun, R. Dhayalan, K. Balasubramaniam, B. Maxfield, P. Peres, D. Barnoncel, An EMAT-based shear horizontal (SH) wave technique for adhesive bond inspection, *Rev. Prog. Quant. Nondestruct. Eval*. **31** (2012) 1268–1275.
[12] D. Ratnam, K. Balasubramaniam, B.W. Maxfield, Generation and detection of higher-order mode clusters of guided waves (HOMC-GW) using meander-coil EMATs, *IEEE Trans. Ultrason. Ferroelectr. Freq. Control* **59** (2012) 727–737.
[13] X. Jian, S. Dixon, R.S. Edwards, J. Morrison, Coupling mechanism of an EMAT, *Ultrasonics* **44** (2006) e653–e656.
[14] R. Dhayalan, K. Balasubramaniam, C.V. Krishnamurthy, Numerical simulation of pulsed meander coil EMAT, *AIP Conf. Proc*. **1211** (2010) 972–979.
[15] R. Murayama, Driving mechanism on magnetostrictive type electromagnetic acoustic transducer for symmetrical vertical-mode Lamb wave and for shear horizontal-mode plate wave, *Ultrasonics* **34** (1996) 729–736.
[16] W.F. Lu, T.C. Chen, K.C. Tsai, T.Y. Yung, The corrosion behavior of carbon steel materials used at nuclear power plants during deactivation and decommissioning processes, *Metals* **14** (2024) 1444.
[17] T. Islam, H.M.M.A. Rashed, Classification and application of plain carbon steels, in: Reference Module in Materials Science and Materials Engineering, Elsevier (2019).
[18] R. Murayama, Non-destructive evaluation of formability in cold rolled steel sheets using the SH0 mode plate wave by electromagnetic acoustic transducer, *Ultrasonics* **39** (2001) 335–343.
[19] R. Dhayalan, K.V. Rajkumar, A. Kumar, Electromagnetic acoustic detection of defects in thick carbon steel plates using high frequency guided waves, *Int. J. Appl. Electromagn. Mech*. (2024) https://doi.org/10.1177/13835416251391591.
[20] C.Z. Sun, A. Sinclair, T. Filleter, Influence of magnetostriction induced by the periodic permanent magnet electromagnetic acoustic transducer (PPM EMAT) on steel, *Sensors* **21** (2021) 7700.
[21] R. Dhayalan, K. Balasubramaniam, A two-stage finite element model of a meander coil electromagnetic acoustic transducer transmitter, *Nondestruct. Test. Eval*. **26** (2011) 101–118.
[22] M. Lowe, B. Pavlakovic, DISPERSE User's Manual and Introduction, Version 2.0.16B, Imperial College, London (2003).
[23] M. Niethammer, L.J. Jacobs, J. Jarzynski, Time-frequency representations of Lamb waves, *J. Acoust. Soc. Am*. **109** (2001) 1841–1847.